


Orlistat facilitates immunotherapy via AKT-FOXO3a-FOXM1-mediated PD-L1 suppression

Qingyun Tang,¹ Jie Li,¹ Lianhua Zhang,¹ Shuo Zeng,¹ Qiyu Bao,¹ Weichao Hu,¹ Lijiao He,¹ Guiping Huang,¹ Liting Wang,² Yunyi Liu,¹ Xiaoyan Zhao,¹ Shiming Yang,¹ Changjiang Hu ¹

To cite: Tang Q, Li J, Zhang L, et al. Orlistat facilitates immunotherapy via AKT-FOXO3a-FOXM1-mediated PD-L1 suppression. *Journal for ImmunoTherapy of Cancer* 2025;**13**:e008923. doi:10.1136/jitc-2024-008923

► Additional supplemental material is published online only. To view, please visit the journal online (<https://doi.org/10.1136/jitc-2024-008923>).

QT, JL and LZ contributed equally.

Accepted 02 December 2024



© Author(s) (or their employer(s)) 2025. Re-use permitted under CC BY-NC. No commercial re-use. See rights and permissions. Published by BMJ Group.

¹Department of Gastroenterology, Army Medical University Xinqiao Hospital, Chongqing, China
²Army Military Medical University, Chongqing, China

Correspondence to

Dr Changjiang Hu;
hcj888@tmmu.edu.cn

Professor Shiming Yang;
yangshiming@tmmu.edu.cn

Dr Xiaoyan Zhao;
zhaoxiaoyan2018@126.com

ABSTRACT

Background The immunotherapy targeting cytotoxic T lymphocyte-associated antigen-4 (CTLA-4) and programmed cell death ligand-1 (PD-L1) has achieved significant breakthroughs, but further improvements are still needed in cancer treatment.

Methods We investigated orlistat, a drug approved by the Food and Drug Administration for the treatment of obesity and found that it can enhance the efficacy of CTLA-4 blockade immunotherapy. We conducted both in vivo and in vitro experiments to explore the mechanism by which orlistat increased antitumor immunity.

Results Orlistat enhances the efficacy of anti-CTLA-4 immunotherapy by suppressing tumor cell PD-L1 protein expression and boosting the transcription of interferon-stimulated genes (ISGs) and MHC-I. Mechanistically, orlistat inhibits AKT activity and subsequent phosphorylation of forkhead box O3a (FOXO3a) at its threonine (T) 32, serine (S) 253, thereby downregulating Forkhead box M1 (FOXM1) expression, which ultimately suppresses PD-L1 transcription. Specifically, inhibition of FOXM1 leads to FOXO3a accumulation through impaired AKT activity. FOXM1 activates protein kinase B (AKT) via acting as a scaffold to facilitate 3-phosphoinositide-dependent protein kinase 1 (PDK1) and AKT and interaction. In addition, orlistat enhances phosphorylated signal transducer and activator of transcription 1 (p-STAT1) at tyrosine (Y) 701, resulting in upregulation of ISGs and MHC-I.

Conclusions Orlistat plays a crucial role in modulating the immune response and supporting the combination with CTLA-4 blockade to promote antitumor immunotherapy.

BACKGROUND

The utilization of immune checkpoint inhibitors has dramatically transformed oncology therapy. Although anti-PD-1/PD-L1 or CTLA-4 antibodies have been approved for the treatment of various cancers, only a fraction of patients experience a durable and effective antitumor immune response, with many patients demonstrating primary resistance.^{1–3} The heterogeneous clinical response to immune checkpoint blockade (ICB) is multifactorial, including tumor-intrinsic and

WHAT IS ALREADY KNOWN ON THIS TOPIC

⇒ Immune checkpoint blockade therapy targeting programmed cell death protein 1 (PD-1)/PD-L1 or CTLA-4 has gained approval for the treatment of various tumor types, providing sustained clinical benefits. However, the effectiveness varies across different cancer types, and the current response rates remain low.

WHAT THIS STUDY ADDS

⇒ We provided evidence that orlistat increases the efficacy of anti-CTLA-4 mAb immunotherapy.
⇒ We proposed that FOXM1 acts as a scaffold protein to promote complex formation between PDK1 and AKT, and that FOXM1 post-transcriptionally down-regulates FOXO3a by activation of AKT signaling.
⇒ We found that orlistat promotes the expression of interferon-stimulated genes and MHC-I by directly binding to STAT1 and activating the STAT1 pathway.

HOW THIS STUDY MIGHT AFFECT RESEARCH, PRACTICE OR POLICY

⇒ This study enhances the understanding of the AKT-FOXO3a-FOXM1-PD-L1 axis and encourages the use of immune checkpoint inhibitors in combination with orlistat as an effective immunotherapy for cancer.

tumor-extrinsic factors.^{4,5} The tumor-intrinsic factors mainly consist of genetic and epigenetic defects and aberrant oncogenic signaling and metabolic pathways.⁴ Mutations that activate phosphatidylinositol-3-kinase (PI3K) are related to an increase in PD-L1 on tumor cells, which results in immune evasion.⁶ Activation of Wnt/β-catenin also results in resistance to ICB by modifying the levels of PD-L1 and programmed cell death ligand-2 (PD-L2) in a diverse set of malignancies.^{7,8} As a result, new approaches have emerged to tackle these challenges and to boost ICB response, including manipulation of epigenetic state, signaling pathways, cytokines, and

antiangiogenic agents, some of which are being evaluated in a number of clinical trials.^{9,10}

Orlistat, an antiobesity medicine licensed by the Food and Drug Administration (FDA), is effective against numerous human cancers, not only due to its capacity to inhibit fatty acid synthase activity, but also because it inhibits tumor cell proliferation, invasion, migration, angiogenesis, and promotes apoptosis.^{11–13} Additionally, orlistat could also stimulate the host's immune system, such as by activating CD8⁺ T cells and natural killer (NK) cells in solid tumors.¹⁴ However, the potential role of orlistat in the modulation of immunotherapy is still poorly understood.

In this study, we found that orlistat improved CTLA-4 blockade immunotherapy by lowering PD-L1 levels and enhancing interferon-stimulated genes (ISGs) and antigen presentation genes expression. In addition, we explored the molecular mechanism underlying AKT-FOXO3a-FOXM1 mediated PD-L1 expression. Our findings highlight orlistat's critical role in modulating immune checkpoint expression and argue for combining orlistat treatment with anti-CTLA-4 therapy to facilitate antitumor immunotherapy.

MATERIALS AND METHODS

Cell culture and transfection

Cells were grown at 37°C in a 5% CO₂ environment in dulbecco's modified eagle medium (Gibco, C11995500BT) containing 10% fetal bovine serum (CellMax, SA211.02), and 1% penicillin/streptomycin (Beyotime, C0222). At 80%–90% confluence, cells were passaged with 0.05% trypsin and 0.02% EDTA (Beyotime). All transfection assays were performed using Lipofectamine 3000 Reagent (Invitrogen) and the medium was changed to complete cell culture media after 6–8 hours of transfection. Transfected cells were examined 36–48 hours after transfection.

RNA extraction and qRT-PCR

Total RNA from human and mouse cell lines and the subcutaneous tumor model was extracted using TRIzol reagent. cDNA was generated from the extracted RNA using a PrimeScript RT reagent kit (Takara). Gene expression was then evaluated using specific primers and the Takara SYBR Green PCR kit with the ABI 7500 Real-Time PCR System (Applied Biosystems). The qRT-PCR primers are listed in Supplementary Table 1.

Chromatin Immunoprecipitation-qPCR

Cells in 10 cm dishes were treated for 36–48 hours before performing Chromatin Immunoprecipitation (ChIP) experiments. The ChIP experiments were conducted strictly according to the protocol from the SimpleChIP Kit (Cell Signaling, #CST 9003S). The following antibodies were used: FOXO3a (D19A7) Rabbit mAb (CST #12829, 1:100 dilution), FOXM1 (D3F2B) Rabbit mAb (CST#20459, 1:100 dilution). The DNA products were

subjected to qRT-PCR analysis, as described above. The primers used for ChIP-qPCR are listed in online supplemental table 1.

Western blot and antibodies

The tumor cells were cultured and treated as indicated. Whole-cell lysates were prepared using RIPA lysis buffer (P0013B, Beyotime, Shanghai, China) containing a protease inhibitor. Prior to loading, protein quantification was performed using an enhanced BCA protein assay kit (P0009, Beyotime, Shanghai, China). As previously mentioned, standard protocols were followed while doing Western blotting (WB).¹⁵ The antibodies used for WB are listed in online supplemental table 2. The original figures of WB are listed in supplemental file 11.

Luciferase reporter assays

Human embryonic kidney 293T (HEK293T) cells were transfected with luciferase reporter vectors, the renilla luciferase (pRL-TK) reporter plasmid, and the corresponding constructs for luciferase reporter experiments. 36 hours after transfection, HEK293T cells were lysed in 100 µL of 1×passive lysis solution, and luciferase activity was determined using the Dual-Luciferase Reporter Assay System (Promega, E1910). Firefly luciferase activity was normalized relative to the co-transfected pRL-TK plasmid.

Co-immunoprecipitation

Cells were lysed on a 4°C shaker for 10 minutes in EBC buffer (50 mM Tris pH 7.5, 120 mM NaCl, and 0.5% NP-40) containing protease inhibitors (4693159001, Roche, Indianapolis, USA). The supernatant was harvested after centrifugation at 13000 rpm at 4°C for 10 min and then incubated with anti-HA (Sigma, A2095), or anti-Flag (Sigma, A2220), or anti-GST agarose beads (ThermoFisher, 16101) at 4°C for 4 hours. The beads containing the immunoprecipitates were washed with NETN buffer (0.5% NP-40, 1 mM EDTA, 20 mM Tris pH 8.0, 150 mM NaCl), and co-immunoprecipitated proteins were analyzed by WB.

Immunohistochemistry

Prior to immunohistochemistry (IHC), paraffin slices were dewaxed with xylene and rehydrated in a series of alcohol solutions of decreasing concentrations. Antigen retrieval was conducted in a high pH solution in a pressure cooker, followed by slowly cooling the samples in the buffer. After inhibiting endogenous peroxidase activity, slices were treated overnight at 4°C with the appropriate antibodies. After counterstaining slides with hematoxylin to highlight cell nuclei for 30–60 s, they were examined under a light microscope.

Surface plasmon resonance

The interaction of STAT1 with orlistat was examined by the surface plasmon resonance (SPR) using the BiaCore 8K biosensor system. pH scouting was performed to determine the optimal pH condition before STAT1 protein was immobilized on the Series S Sensor chip CM7 (Cytiva,

28953828). According to the BiaCore 8K's operating instructions, the chip was first treated with a mixture of 1-ethyl-3-(3-dimethylaminopropyl)-carbodiimide and N-hydroxysuccinimide at a flow rate of 5 μ L/min. Following activation, STAT1 (TargetMol, TMPJ-00961) was immobilized on the sensor chip surface using a sodium acetate buffer (pH 5.0). Ethanolamine was used to inactivate the remaining carboxymethylated active residue of the sensor chip. Each analyte was dissolved in 1×HBS-N buffer (Cytiva, BR100670), containing 0.05% Tween 20. Four-point solvent correction and twofold diluted samples for binding assay in 2% dimethyl sulfoxide (DMSO) were performed. Sensorgrams were recorded and analyzed using Biacore Insight Evaluation Software.

Animal experiments

Animal experiments were approved by the ethics committee of the Army Medical University. The housing conditions included controlled temperature, humidity, and a 12-hour light/dark cycle, with unrestricted access to food and water. All experimental animals were assigned to groups using a simple randomization method. Huafukang Biotechnology Company (Beijing, China) provided female C57BL/6 mice ranging in age from 5 to 6 weeks. For orlistat/CTLA-4 mAb combination treatment, C57BL/6 mice were randomly divided into four treatment groups: control, orlistat, CTLA-4 mAb, and CTLA-4 mAb with orlistat. As illustrated in [figure 1B](#), mice were inoculated subcutaneously with 5×10^5 MC38 cells in the right flank near the thigh root of the mice. From the fifth day of tumor inoculation, the orlistat (50 mg/kg) (MCE HY-B0218, formulated in 10% DMSO, 40% PEG400, 5% Tween-80, 45% saline) was administered daily via intraperitoneal injection for 21 days. CTLA-4 mAb was injected intraperitoneally at a dose of 200 μ g every 3 days for a total of 3 injections, beginning on day 7 after tumor inoculation. Thereafter, tumor volume of all the mice was measured every 3 days from days 7 until 60 days. The formula used to determine the tumor volume was tumor volume = $1/2 \times (\text{length} \times \text{width} \times \text{width})$. Survival curves were estimated using the Kaplan-Meier method. For the subcutaneous MC38 model, C57BL/6 mice were implanted with subcutaneous MC38-WT cells (5×10^5 cells) in the left flank near the thigh root of the mice and MC38 shFOXMI cells (5×10^5 cells) in the symmetrical position on the right flank.

For the combination treatment of orlistat and CTLA-4 mAb, with or without PD-L1 mAb, as illustrated in (online supplemental figure S2I) online supplemental figure S2G), orlistat and CTLA-4 mAb were administered as previously described. PD-L1 mAb was injected intraperitoneally at a dose of 100 μ g every 3 days for a total of 3 injections.

For the in vivo xenograft assay, 4–6-week-old female BALB/cNj-Foxn1nu/Gpt mice (Strain No. D000521) were purchased from GemPharmatech (Nanjing, China). AGS cells (2×10^6 cells) were injected subcutaneously into the right flanks of the mice. Orlistat and control

treatments were administered intraperitoneally at a dose of 50 mg/kg every day, starting on day seven after tumor inoculation and continuing until the harvest on day 15.

The detailed methods for Fluorescence-Activated Cell Sorting (FACS) analyses, generation of the CRISPR-mediated FOXM1 knockout cell line, thermal shift assay, In Vitro Kinase Assay, tissue microarray and Multiplexed immunofluorescence, RNA sequencing and data analysis are provided in online supplemental materials and methods.

Statistical analysis

The measurement of mouse volume and statistical analysis of the data were conducted by a designated individual who was blinded to the group assignments. All the statistical data were analyzed by Prism V.9.0. Two-tailed, unpaired t-test or one-way analysis of variance (ANOVA) was applied for comparing normally distributed data. A two-way ANOVA was applied in the tumor growth curve, with Tukey's multiple comparisons test between the values in each group. The survival analysis utilized the log-rank test based on the Kaplan-Meier survival analysis. FACS data were analyzed with FlowJo software V.10.10. WB bands quantitative analysis was measured by Image J software in at least three independent immunoblots first normalized to corresponding loading controls and then to the first controls. Error bars show SD. * $p < 0.05$, ** $p < 0.01$, *** $p < 0.001$. ns, no significance.

RESULTS

Orlistat sensitizes tumors to CTLA-4 mAb ICB therapy

Orlistat has been found to inhibit tumor progression in a variety of malignancies. Recent research demonstrates that orlistat induces anticancer immune response by promoting the development of intratumoral dendritic cells (DCs) and the effector function of CD8⁺ T cells and NK cells.¹⁴ Next, we investigated the potential role of orlistat in CTLA-4 mAb blockade therapy. We administered orlistat and/or anti-CTLA-4 antibody to syngeneic mice carrying MC38 tumors ([figure 1A,B](#)). The combination therapy significantly decreased tumor development and resulted in the survival of seven out of twelve mice ([figure 1A](#)). In addition, mice treated with a combination of orlistat and CTLA-4 mAb exhibited better overall survival compared with those given either medication alone ([figure 1C](#)) and had smaller tumor sizes ([figure 1D](#)). To decipher the mechanism of combination therapy-suppressed tumor growth, tumor-infiltrating T lymphocytes (TILs) were isolated and examined by FACS for the proportions of immune cell populations within tumors on day 15, when tumors were similar in volume ([figure 1D](#)). More tumor-infiltrating CD8⁺ T cells, but not CD4⁺ T cells, and increased production of the effector molecules Granzyme B (GZMB), interferon (IFN) γ , and tumor necrosis factor (TNF) α production were found in the tumors of the combination-treatment group ([figure 1F–J](#)). Consistent with these findings, the increased

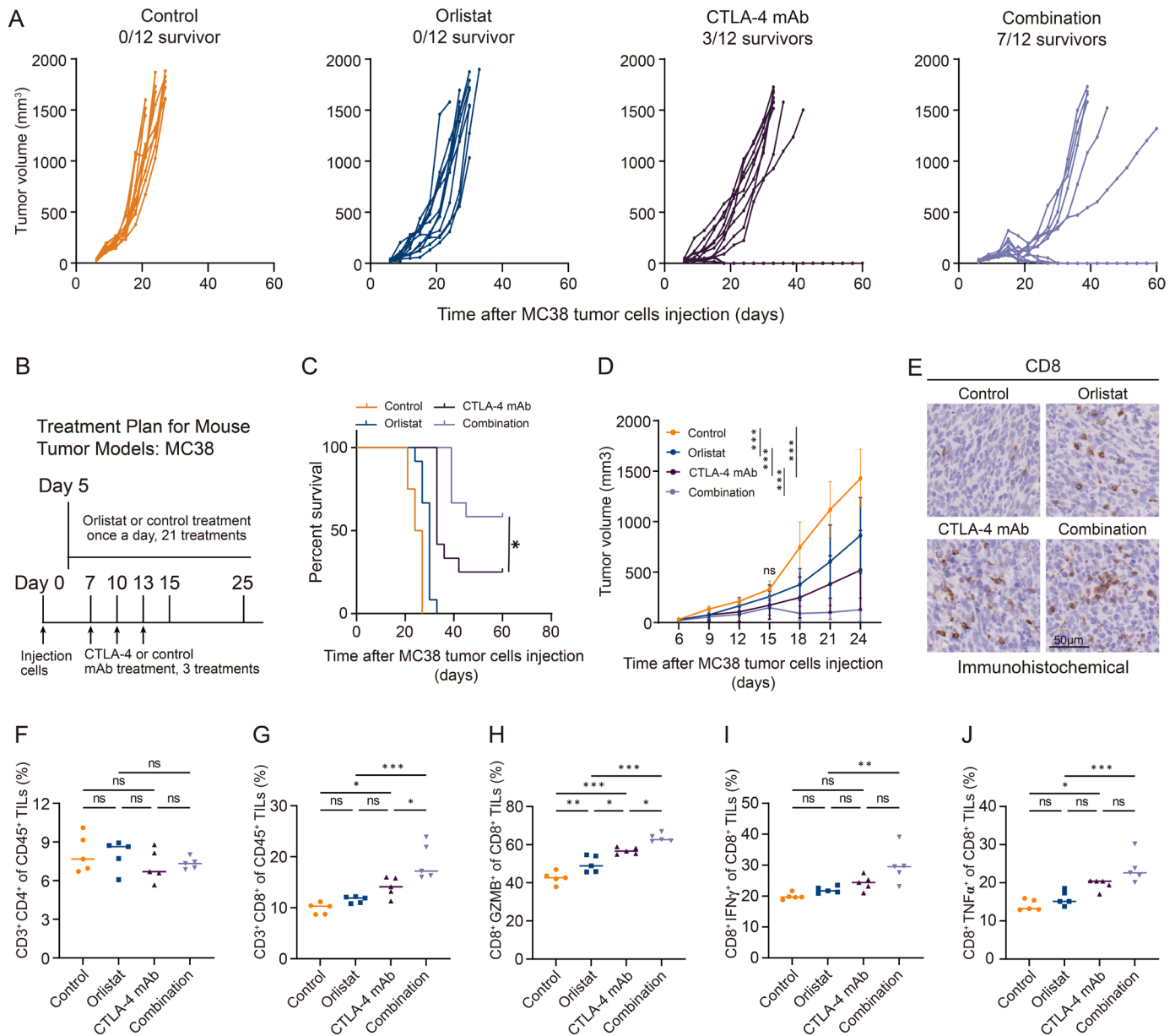


Figure 1 Orlistat sensitizes tumors to CTLA-4 mAb ICB therapy. (A) Tumor volume curves of MC38 tumor-bearing mice treated with the designated treatments. Tumor volumes were monitored every 3 days by measuring tumor diameters (n=12 in each group). (B) A schematic illustration of the treatment schedule of tumor-bearing mice for figure 1A,C. (C) Kaplan-Meier survival curves of mice in the different treatment groups (n=12). (D) Tumor growth curves of WT C57BL/6 mice inoculated with 10⁵ MC38. (E) Representative images of MC38 tumors immunohistochemically stained for CD8. Scale bar=50μm. (F–G) FACS analysis of cell proportions of CD3⁺CD4⁺ (F) and CD3⁺CD8⁺ out of CD45⁺ TILs (G). (H–J) CD8⁺GZMB⁺ (H), CD8⁺IFNγ⁺ (I), and CD8⁺TNFα⁺ (J) out of CD8⁺ TILs from MC38-implanted tumors (n=5 in each group). ICB, immune checkpoint blockade. *p<0.05, **p<0.01, ***p<0.001. ns, no significance

CD8 protein was also confirmed by IHC compared with untreated controls (figure 1E). Collectively, these data demonstrate that combining orlistat treatment with immunotherapy targeting CTLA-4 dramatically enhances tumor regression.

Orlistat downregulates PD-L1 expression both in vitro and in vivo

To further investigate how orlistat enhances the anti-tumor effects of CTLA-4 blockade, we examined the proportion of other immune cells in the tumor. We

found that after orlistat treatment, there were no significant alterations in the proportion of CD11b⁺ myeloid cells. Additionally, the proportions of DCs, granulocytic myeloid-derived suppressor cells (G-MDSCs), monocytic MDSCs (M-MDSC), and macrophage cells (MCs), were similar between the two groups (online supplemental figure S1A–E). Similarly, no significant changes were observed in the lymphocytes from the spleen and draining lymph nodes (online supplemental figure S1F, G). All these data indicate that orlistat sensitizes tumors to

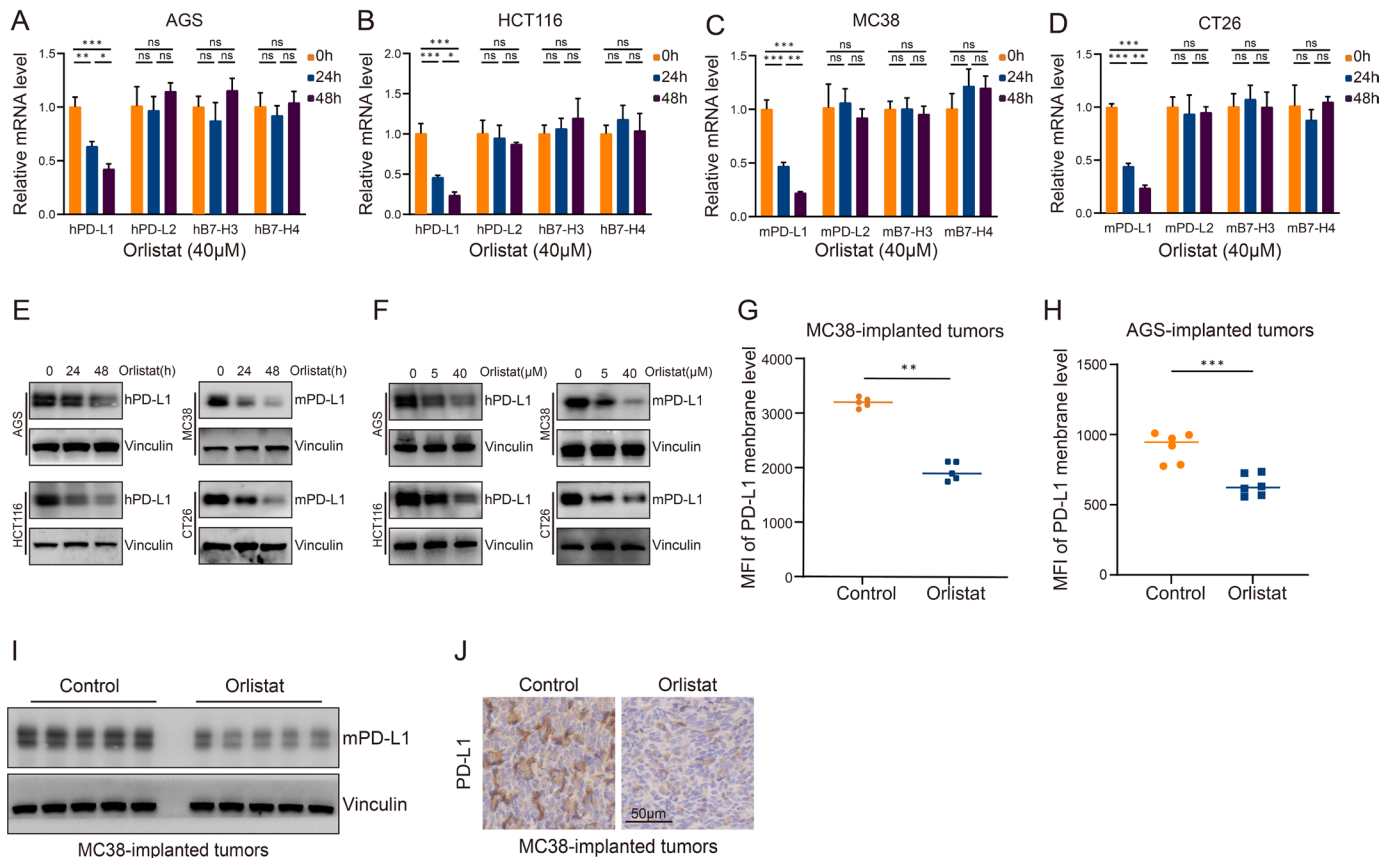


Figure 2 Orlistat downregulates PD-L1 expression both in vitro and in vivo. (A–D) RT-PCR measurement of mRNA expression of PD-L1, PD-L2, B7-H3, and B7-H4 after orlistat (40 μM) treatment for 0 hour, 24 hours, or 48 hours in AGS, HCT116, MC38, and CT26 cells. (E) Expression of PD-L1 protein in AGS, HCT116, MC38 and CT26 cells at different times (0 hour, 24 hours, 48 hours) after orlistat administration. (F) Western blot (WB) analysis of PD-L1 protein levels after orlistat administration at different dosing strategies (0, 5, 40 μM) in AGS, HCT116, MC38, and CT26 cells. (G, H) FACS analysis of mean fluorescence intensity (MFI) of PD-L1 from MC38-implanted tumors (n=5 mice in each group) (G) and AGS-implanted tumors (n=6 mice in each group) (H); tumor-bearing mice were treated with vehicle or orlistat for 11 days. (I) WB detection of PD-L1 expression on tumors collected from mice bearing subcutaneous MC38 tumors with or without orlistat treatment. (J) PD-L1 immunohistochemistry performed on tumor tissue from MC38 tumor-bearing mice treated with control or orlistat treatment. Scale bar=50 μm. *p<0.05, **p<0.01, ***p<0.001. ns, no significance.

CTLA-4 mAb ICB therapy neither by altering the proportion of myeloid suppressor cells in tumor microenvironment nor T lymphocytes in secondary lymphoid organs. The combination therapy of PD-L1 and CTLA-4 ICB enhances antitumor effects.^{3,16} We investigated whether orlistat enhances CD8⁺ T cell infiltration in tumors by modulating the expression of PD-L1 on the surface of tumor cells. Next, the expression of B7 family checkpoint proteins on tumor cells was evaluated, including PD-L1, PD-L2, B7 homolog 3 (B7-H3), and B7 homolog 4 (B7-H4).^{17,18} The results showed that orlistat suppressed PD-L1 mRNA in AGS, HCT116, MC38, and CT26 cells in a time and dose-dependent manner, without obvious change of PD-L2, B7-H3, and B7-H4 mRNA levels (figure 2A–D and online supplemental figure S2A, B). Moreover, orlistat decreased PD-L1 protein abundance in the above cell lines (figure 2E,F and online supplemental figure S2C, D), suggesting that orlistat suppresses PD-L1 expression via transcriptional regulation. This is consistent with prior studies showing that orlistat decreases PD-L1 expression

in cisplatin-resistant bladder cancer cells and human T-cell leukemia lines.^{19,20} To further examine the effect of orlistat on PD-L1 expression in vivo, FACS was employed to determine the PD-L1 levels on the tumor cell surface of C57BL/6 mice implanted with MC38 tumors as well as nude mice implanted with AGS tumors. figure 2G,H reveals that orlistat significantly attenuated PD-L1 expression in tumors collected from orlistat-treated mice compared with control mice. In agreement with the FACS analysis results, orlistat dramatically suppressed PD-L1 expression compared with control samples in the MC38 syngeneic graft model, as demonstrated by WB and IHC (figure 2I,J and online supplemental figure S2E). Additionally, orlistat decreased PD-L1 protein in mouse organs, including small intestines, livers, and thymi (online supplemental figure S2F–H). We next sought to corroborate that orlistat enhances the efficiency of CTLA4 mAb treatment by downregulating PD-L1 expression. The efficacy of orlistat and anti-CTLA-4 therapy alone or in combination with PD-L1 mAb was analyzed by FACS (online supplemental

figure S2I). The results showed that the addition of anti-PD-L1 did not significantly improve the proportions and function of CD8⁺ T cells compared with the orlistat combined with CTLA-4 mAb group (online supplemental figure S2J-N). These results together suggest that orlistat decreases PD-L1 expression both in vitro and in vivo.

Orlistat suppresses PD-L1 via inhibition of FOXM1 signaling

Next, we attempted to determine the mechanism by which orlistat reduces PD-L1 expression. Considering the inhibitory effects of orlistat on PD-L1 mRNA, we reasoned that orlistat might affect transcription factors, especially those that have been reported to regulate PD-L1. RNA sequencing was then performed on MC38-bearing mice treated with orlistat or control DMSO. Subsequently, we ranked the well-demonstrated transcription factors that regulate the expression of PD-L1 in the RNA-seq results.^{21–25} Interestingly, FOXM1 was the most downregulated transcription factor after orlistat administration ($\log_2FC = -0.34$), suggesting it as a potential downstream effector regulated by orlistat (figure 3A). Orlistat induced a time and dose-dependent downregulation of FOXM1 mRNA and protein expression in different cancer cell lines (figure 3B–D and online supplemental figure S3A–E). Moreover, the immunohistochemical analysis showed that the abundance of FOXM1 was substantially decreased after orlistat treatment (figure 3E). Together, these results imply that orlistat transcriptionally downregulates FOXM1.

Previous studies have reported that FOXM1 promotes PD-L1 expression in lung cancer cells by interacting directly with the PD-L1 promoter.²⁴ Our results also revealed that FOXM1 increased the PD-L1 mRNA and protein levels, whereas knockdown of FOXM1 significantly reduced PD-L1 mRNA and protein levels in different cancer cells (figure 3F,G and online supplemental figure S3F). Furthermore, ChIP-qPCR revealed that FOXM1 is bound to the PD-L1 promoter at the (+222 to +450 bp) region (figure 3H,I). Orlistat inhibited FOXM1 binding to the PD-L1 promoter and simultaneously reversed FOXM1-enhanced PD-L1 promoter activity (figure 3J,K). To further prove whether FOXM1 regulated PD-L1 in mice, MC38 cell lines with stable knockdown of FOXM1 were constructed. WT mice were injected with short hairpin RNA negative control (shControl) as a negative control or short hairpin RNA targeting FOXM1 (shFOXM1) to generate a syngeneic subcutaneous tumor model. WT mice implanted with MC38 cells with shFOXM1 had smaller tumor sizes and weight than those implanted with shControl (online supplemental figure S3G–H) (online supplemental figure S3H, I), confirming the tumor-promoting role of FOXM1. FACS analysis indicated that the proportion of CD8⁺ T cells was significantly increased in shFOXM1 tumor tissues (online supplemental figure S3I) (online supplemental figure S3J), and WB demonstrated that PD-L1 expression was diminished in shFOXM1 tumor tissue (online supplemental figure S3J) (online supplemental figure S3K).

These results indicate that FOXM1 promotes PD-L1 expression and reduces tumor-infiltrating CD8⁺ T cells in vivo. Furthermore, we generated a FOXM1^{−/−} AGS cell line using CRISPR/Cas9 technology, and its efficiency was confirmed by genome sequencing (online supplemental figure S3K) (online supplemental figure S3L). In FOXM1-depleted cells, PD-L1 was significantly decreased. More importantly, the orlistat-mediated suppression of PD-L1 was almost abolished in FOXM1 knockout cells (supplemental figure S3L) (online supplemental figure S3G), supporting the important role of FOXM1 in orlistat-mediated downregulation of PD-L1.

Orlistat-suppressed PD-L1 depends on AKT-FOXO3a-FOXM1 signaling

To identify the downstream pathways affected by orlistat treatment, RNA-seq was performed on purified syngeneic graft MC38 tumor cells with or without orlistat. According to GSEA analysis, immune-related pathways and PI3K-AKT signaling pathways were enriched (figure 4A,B). AKT phosphorylates FOXO3a at its T32, S253, and S315 sites, and FOXO3a has been shown to downregulate FOXM1 transcription.^{26–29} Therefore, we hypothesized that orlistat's suppression of PD-L1 transcriptional activation may be mediated by the AKT/FOXO3a/FOXM1 pathway. Thermal shift assay demonstrated that orlistat enhanced the thermal stability of AKT, indicating the protein interaction between AKT and orlistat (figure 4C). Furthermore, orlistat administration reduced phosphorylated AKT (p-AKT) and phosphorylated FOXO3a (p-FOXO3a) in a time-dependent and dose-dependent manner in multiple cancer cell lines with elevated FOXO3a expression (figure 4D, online supplemental figure S4A, B). Additionally, p-AKT T308, p-AKT S473, p-FOXO3a S253, and p-FOXO3a T32 were diminished with increased FOXO3a abundance in tumors and various organs of orlistat-treated mice compared with controls (figure 4E,F, online supplemental figure S4C–F). IHC confirmed that FOXO3a expression was upregulated in response to orlistat treatment (figure 4G). Co-administration with CTLA-4 mAb did not affect the impact of orlistat on AKT/FOXO3a/FOXM1 proteins (online supplemental figure S4G) but increased the expression of PD-L1, possibly because CTLA-4 antibody therapy activates immune responses, which leads to the upregulation of PD-L1 expression on tumor cells as a feedback mechanism to balance and evade the host immune attack.³ Specifically, overexpression of FOXO3a decreased the PD-L1 expression (figure 4H and online supplemental figure S4H), whereas knockdown of FOXO3a expression of elevated the PD-L1 expression (figure 4I and online supplemental figure S4I). Notably, orlistat suppressed PD-L1 protein levels were significantly rescued in FOXO3a knockdown AGS and HCT116 cells (figure 4J and online supplemental figure S4J), demonstrating that orlistat inhibited PD-L1 levels in a FOXO3a-dependent manner. To verify whether FOXO3a regulates the levels of PD-L1 in a FOXM1-dependent manner, we knocked

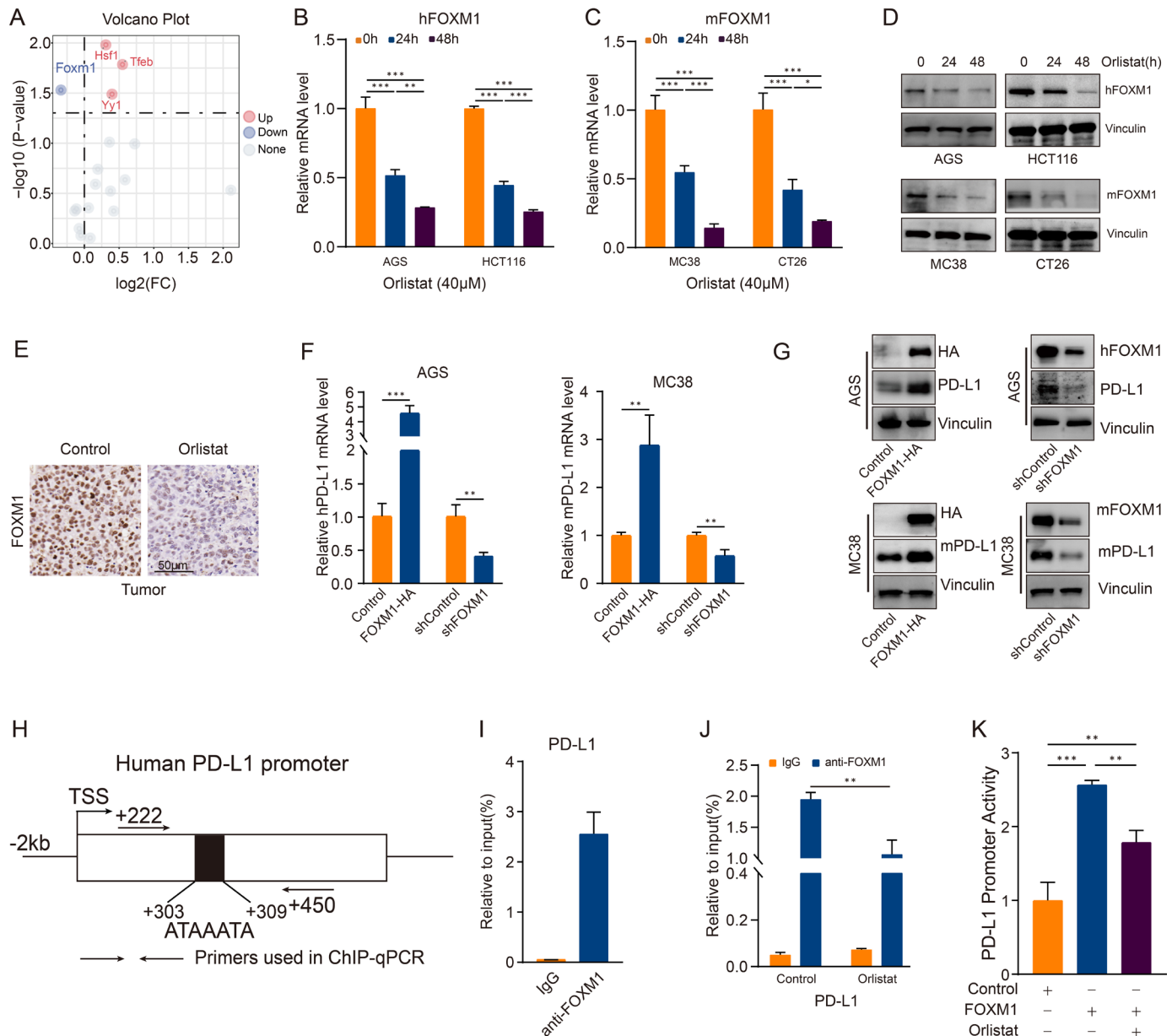


Figure 3 Orlistat suppressed PD-L1 via inhibition of FOXM1 signaling. (A) Volcano plot of the expression of the reported transcription factors that regulated the expression of PD-L1. These TFs include STAT1, ATF3, IRF2, TFEB, IRF1, YY1, STAT3, JUN, HSF1, NF κ B, SP1, FOXP3, BRD4, EZH2, MYC, HIF-1 α , and FOXM1. (B, C) qRT-PCR measurement of mRNA expression of FOXM1 after orlistat (40 μ M) treatment for 0 hour, 24 hours, or 48 hours in AGS and HCT116 (B), MC38 and CT26 cells (C). (D) WB analysis of FOXM1 protein levels after orlistat treatment for different times (0 hour, 24 hours, 48 hours) in AGS, HCT116, MC38, and CT26 cells. (E) Representative images of immunohistochemical staining of FOXM1 protein expression in resected tumors at day 25. Scale bar=50 μ m. (F) The expression of PD-L1 mRNA in AGS and MC38 cells after transfection with FOXM1 overexpression or knockdown. (G) WB for PD-L1 protein levels after FOXM1 overexpression or knockdown in AGS and MC38 cells. (H) Schematic representation of the PD-L1 gene promoter regions and primer pairs used for ChIP assays. (I) ChIP-qPCR assay was used to detect the binding of FOXM1 to the PD-L1 promoter at the (+222 to +450 bp) region in AGS cells. (J) ChIP-qPCR analysis of the impact of orlistat (40 μ M) on the binding of FOXM1 to the PD-L1 promoter. (K) The luciferase activity of PD-L1 promoter after FOXM1 overexpression with or without orlistat (40 μ M). HEK293T cells in 24-well plates were transfected with FOXM1 plasmids or control. The luciferase activity was measured 36 hours later. * p <0.05, ** p <0.01, *** p <0.001.

down FOXO3a in FOXM1-deficient AGS cells and found that FOXO3a-suppressed PD-L1 expression was almost abolished once FOXM1 knocked out (figure 4K and online supplemental figure S4K). These results illustrate that orlistat inhibits PD-L1 expression through modulation of the AKT/FOXO3a/FOXM1 pathway.

FOXO3a transcriptionally regulates FOXM1 in cancer cells

Recent studies have suggested that FOXO3a negatively regulates FOXM1 transcription in breast and cervical cancers.²⁷⁻²⁹⁻³¹ We, therefore, evaluated whether FOXO3a affects FOXM1 signaling in our system. Overexpression of FOXO3a dramatically decreased FOXM1 mRNA and

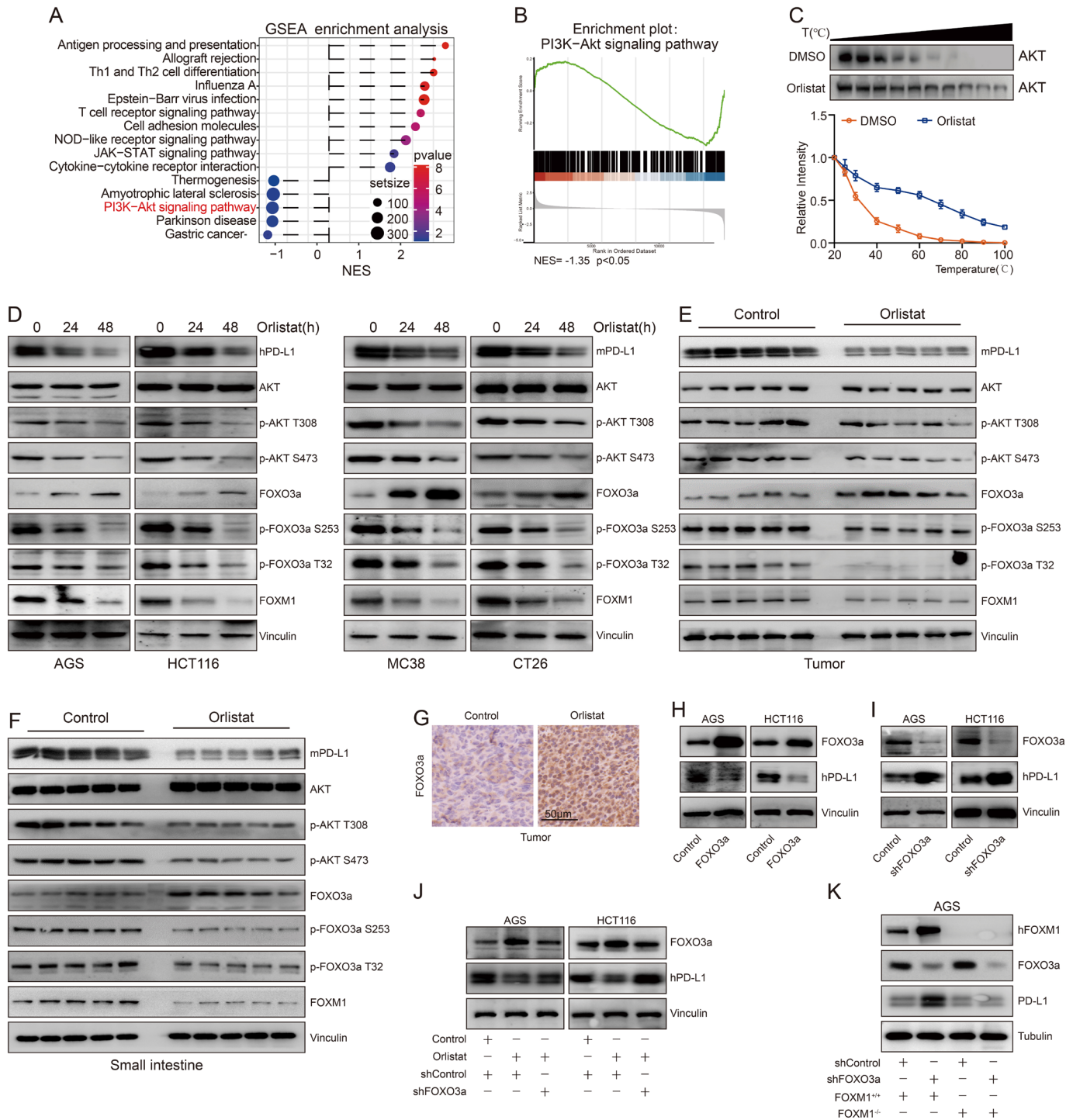


Figure 4 Orlistat-suppressed PD-L1 depends on AKT-FOXO3a signaling. (A) Enrichment plots from gene set enrichment analysis (GSEA) in MC38 tumors from mice treated with vehicle or orlistat. (B) GSEA plots for the PI3K-AKT signaling pathway. (C) Stabilization of AKT by orlistat (40 µM) using a cellular thermal shift assay. (D) AGS, HCT116, MC38, and CT26 cells were treated with orlistat (40 µM) for the indicated times (0 hour, 24 hours, 48 hours) before harvesting for WB analysis. (E, F) MC38 tumors-bearing C57BL/6 mice were treated with vehicle or orlistat for 21 days; then, tumors (E) and small intestines (F) were collected for IB analysis. (G) Representative immunohistochemistry images of FOXO3a protein expression in MC38 tumor-bearing mice. Scale bar=50 µm. (H, I) WB analysis of the effect of FOXO3a overexpression (H) and knockdown (I) on PD-L1 expression in AGS and HCT116 cells. (J) AGS and MC38 cells transfected with shFOXO3a or shControl (used as a negative control) plasmids were treated with orlistat or vehicle. Protein expression levels of FOXO3a and PD-L1 were measured. (K) FOXM1 WT or knockout AGS cells transfected with shControl or shFOXO3a plasmids were treated with orlistat (40 µM) for 48 hours before harvesting for IB analysis.

protein levels (figure 5A,B and online supplemental figure S5A). Furthermore, suppression of FOXO3a led to a considerable rise in the mRNA and protein levels of FOXM1 in gastric cancer cells (figure 5C,D and online supplemental figure S5B). Subsequently, dual luciferase reporter assays illustrated that the knockdown of FOXO3a significantly enhanced the promoter activity of FOXM1 (figure 5E). Studies with truncated promoter constructs identified that the FOXO3a response element was located in the FOXM1 promoter region (−1975 to −581 bp) (figure 5F,G). ChIP-qPCR confirmed that FOXO3a directly bound to the FOXM1 promoter region FHRE (forkhead response element) two but not to the region FHRE1 (figure 5H,I). Further studies demonstrated that orlistat promoted the binding of FOXO3a to the FOXM1 promoter, while it reversed the enhancement of FOXM1 promoter activity induced by shFOXO3a (figure 5J,K). These findings demonstrate that FOXO3a directly binds to the FHR2 region of the FOXM1 gene promoter to inhibit FOXM1 transcription.

FOXM1 promotes the phosphorylation of FOXO3a through AKT activation

Interestingly, we confirmed that overexpression of FOXM1 decreased FOXO3a protein without influencing FOXO3a mRNA (figure 6A,B and online supplemental figure S5C), whereas knockdown of FOXM1 increased the FOXO3a protein but not mRNA expression (figure 6C,D and online supplemental figure S5D). Figure 6E shows that FOXM1 did not affect FOXO3a promoter activity levels in HEK293T cells. Previous study clearly showed that FOXO3a protein abundance was regulated by PI3K/AKT, extracellular signal-regulated kinase/mitogen-activated protein kinase (ERK/MAPK), and AMP-activated protein kinase (AMPK) pathways.^{26 32} It is well established that FOXO3a is directly phosphorylated by AKT kinase at two conserved sites (T32 and S253).³³ FOXM1 overexpression resulted in increased p-FOXO3a at residues S253 and T32, whereas FOXM1 knockdown reduced p-FOXO3a (S253 and T32) levels; however, FOXM1 did not affect the levels of p-FOXO3a at residues S294, S413, and S425 (figure 6F and online supplemental figure S5E), which are phosphorylated by ERK or AMPK kinase.^{34 35} We further assessed the levels of p-AKT, p-ERK, and p-AMPK. FOXM1 enhanced the phosphorylation of AKT at T308 and S473, but not that of p-AMPK and p-ERK (figure 6G and online supplemental figure S5F), while knockdown of FOXM1 reduced the p-AKT (T308 and S473) levels (figure 6H and online supplemental figure S5G). These conclusions were further supported by the AKT inhibitor MK-2206 2HCl, which almost abolished FOXM1-inhibited FOXO3a protein expression (figure 6I and online supplemental figure S5H).

FOXM1 enhances AKT-PDK1 interaction for AKT activation

We then investigated the molecular mechanism through which FOXM1 stimulates AKT kinase in cells. PI3K/PDK1 is the key upstream regulator of the AKT pathway,

phosphorylating AKT at T308 to activate it.^{36 37} In vitro kinase assays revealed that FOXM1 stimulated AKT kinase activity on purified glycogen synthase kinase three beta (GSK3 β) protein (figure 7A), a downstream substrate of AKT.^{36 38} In addition, co-immunoprecipitation (Co-IP) assays showed that FOXM1 facilitated the binding of PDK1 to AKT in vivo (figure 7B). FOXM1 likely acts as a scaffold protein to facilitate the interaction between AKT and PDK1. Further analysis indicated that orlistat did not impact the interaction between FOXM1 and PDK1-AKT (online supplemental figure S6A). To that end, we detected an interaction between FOXM1 and AKT (figure 7C) and the binding of FOXM1 to PDK1 by Co-IP experiments (figure 7D). To further investigate the detailed protein regions that mediated the FOXM1-AKT and FOXM1-PDK1 interaction, we constructed a series of truncated mutations (online supplemental figure S6B–D). Our experiments suggested that the C-terminal of FOXM1 bound to the AKT pleckstrin-homology (PH) domain and PDK1 N-terminal, respectively (figure 7E–H). Taken together, we demonstrate that FOXM1 enhances AKT activity through the promotion of the PDK1 with AKT interaction.

Orlistat upregulates ISGs and MHC-I through activating the STAT1 pathway

It is well established that antigen presentation pathways, which can be activated by the interferon signaling pathway, also influence the ICB efficacy.^{39–41} To interrogate the effect of orlistat on antigen presentation, RNA-seq was performed on purified tumor cells isolated from mice carrying the MC38 tumor. GO and KEGG pathways enrichment analysis showed that antigen presentation-related pathways such as ‘type I interferon signaling pathway’, ‘antigen processing and presentation’, and ‘JAK-STAT signaling pathway’ were enriched in the orlistat-treated group (figure 8B, online supplemental figure S7A, B). Given that the JAK-STAT signaling pathway was substantially enriched in figure 8B and STAT1 is a key mediator of both type I and II interferon signaling,^{42–44} we evaluated protein levels in purified MC38 tumor bearing cells, MC38 cell lines, and AGS cell lines, finding that orlistat significantly upregulated total STAT1 and p-STAT1 (Y701) protein levels (figure 8C–E, online supplemental figure S7C–E), and this effect was independent of type I IFNs (online supplemental figure S8F, G), indicating that orlistat does not affect the upstream of interferon receptors. The phosphorylated STAT1 proteins move to nucleus, bind specific DNA elements, regulate the transcription of downstream genes, such as ISGs and MHC-I, and simultaneously promote IFNs autocrine.^{42 45–48} Then, we observed an increase in the mRNA transcription of type I IFNs, ISGs, and antigen processing and presentation genes following orlistat administration in purified MC38 bearing tumors, as well as in MC38 and AGS cell lines (figure 8F–J). Further analysis using flow cytometry revealed that orlistat promotes MHC-I membrane expression in AGS and MC38 cell

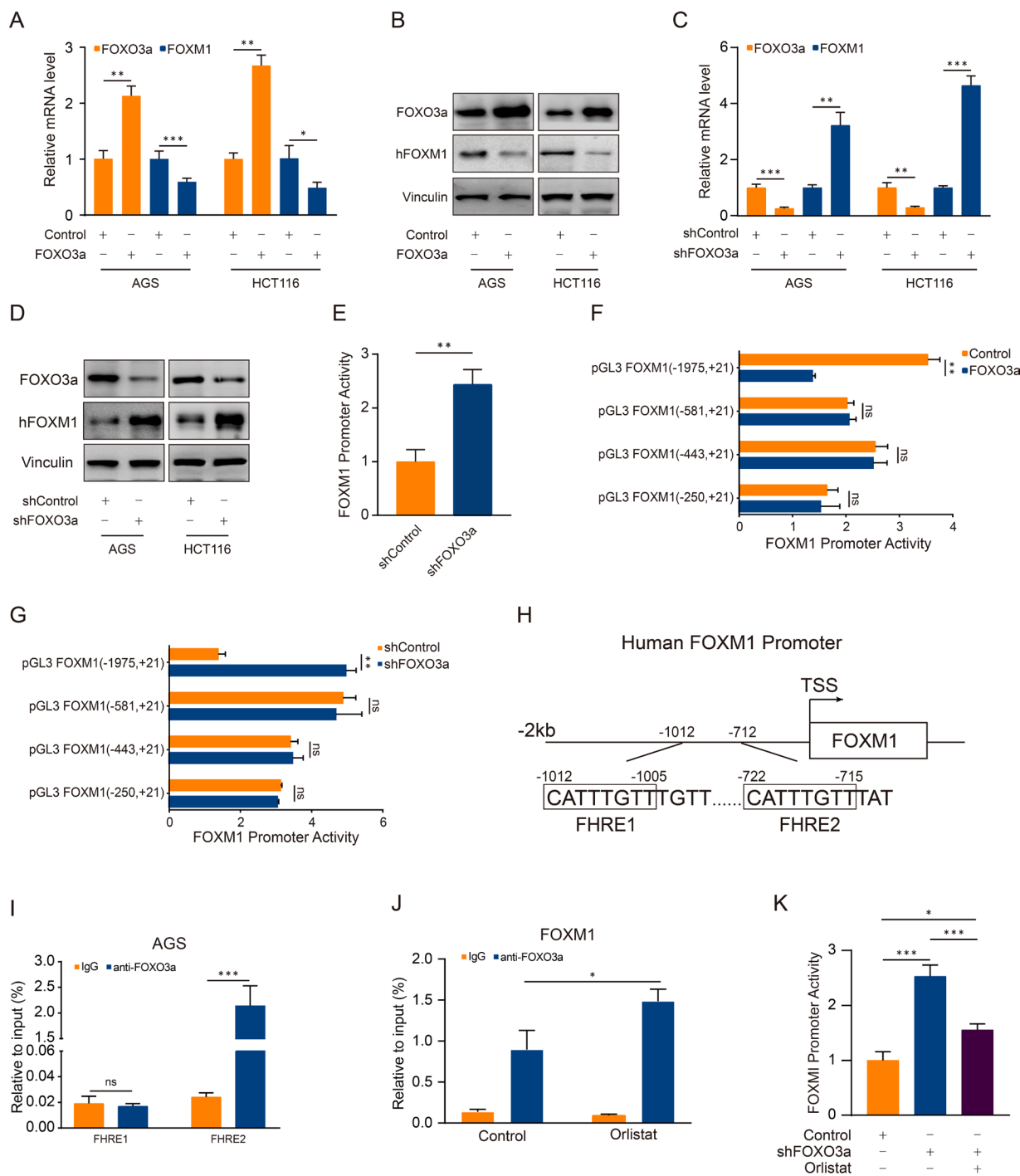


Figure 5 FOXO3a transcriptionally downregulates FOXM1 in cancer cells. (A) Relative expression of FOXM1 was detected by qRT-PCR after RNA extraction from AGS and HCT116 cells transfected with FOXO3a for 48 hours. Each column represents the mean of triplicates. (B) WB analysis of FOXO3a, FOXM1, and Vinculin in AGS and HCT116 cells. The cells were infected with FOXO3a plasmids and the corresponding control plasmids. (C, D) qRT-PCR assay for FOXM1 mRNA (C) and WB analysis for FOXM1 protein levels (D) after knockdown of FOXO3a in AGS or HCT116 cells transfected with either shControl or shFOXO3a plasmids. (E) The luciferase activity of FOXM1 promoter after FOXO3a knockdown. HEK293T cells in 24-well plates were transfected with shFOXO3a plasmids or control. The luciferase activity was measured 36 hours later. (F, G) HEK293T cells were transfected with different recombinant luciferase reporter constructs as indicated together with overexpression (F) or knockdown (G) of FOXO3a. The HEK293T were harvested 36 hours and assayed for luciferase activity. (H) Schematic representation of FOXM1 promoter showing the putative FOXO3a binding sites forkhead response element (FHRE1 and FHRE2) and the position of primers used in ChIP analysis. (I) ChIP-qPCR assays were performed using chromatin isolated from gastric cancer cells infected with lenti-FOXO3a (a lentiviral vector expressing FOXO3a) or lenti-Control (a control lentiviral vector). Final DNA extractions were qPCR amplified using primers that cover FOXM1 binding element (CATTGTT) within the FOXO3a gene. (J) ChIP-qPCR analysis of the impact of orlistat on FOXO3a binding to the FOXM1 promoter. (K) The luciferase activity of FOXM1 promoter after FOXO3a knockdown with orlistat or not. * $p < 0.05$, ** $p < 0.01$, *** $p < 0.001$. ns, no significance.

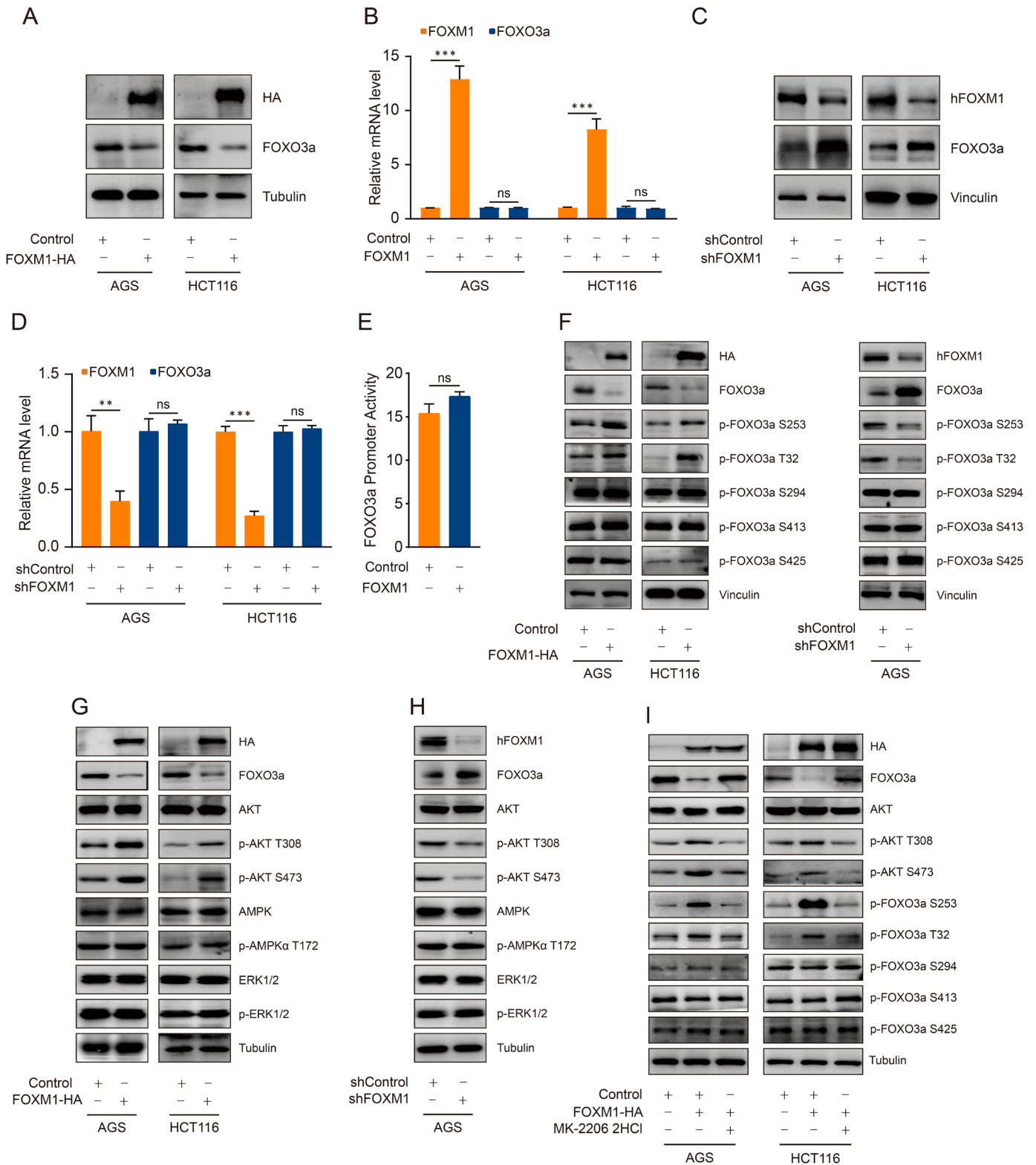


Figure 6 FOXM1 promotes the phosphorylation of FOXO3a through AKT activation. (A, C) WB analysis of the FOXM1 and FOXO3a proteins after overexpression (A) or knockdown (C) of FOXM1 in AGS and HCT116 cells. (B, D) qRT-PCR assay for FOXM1 and FOXO3a mRNA after overexpression (B) or knockdown (D) of FOXM1. (E) Analysis of FOXO3a promoter activity by overexpression of FOXM1. (F) Effects of FOXM1 overexpression or knockdown on the regulation of total FOXO3a and phosphorylated FOXO3a (S253, T32, S294, S413, and S425) levels. (G, H) WB analysis for the AKT, ERK, and AMPK pathways with FOXM1 overexpression or knockdown in AGS and HCT116 cells. (I) FOXM1 overexpressing AGS and HCT116 cells were treated with MK-2206 2HCl (10 μ M) or DMSO control for 36 hours, the protein levels of phosphorylated AKT (p-AKT at T308 and S473), phosphorylated FOXO3a (S253, T32, S294, S413, and S425) were detected by WB. ** $p < 0.01$, *** $p < 0.001$. ns, no significance.

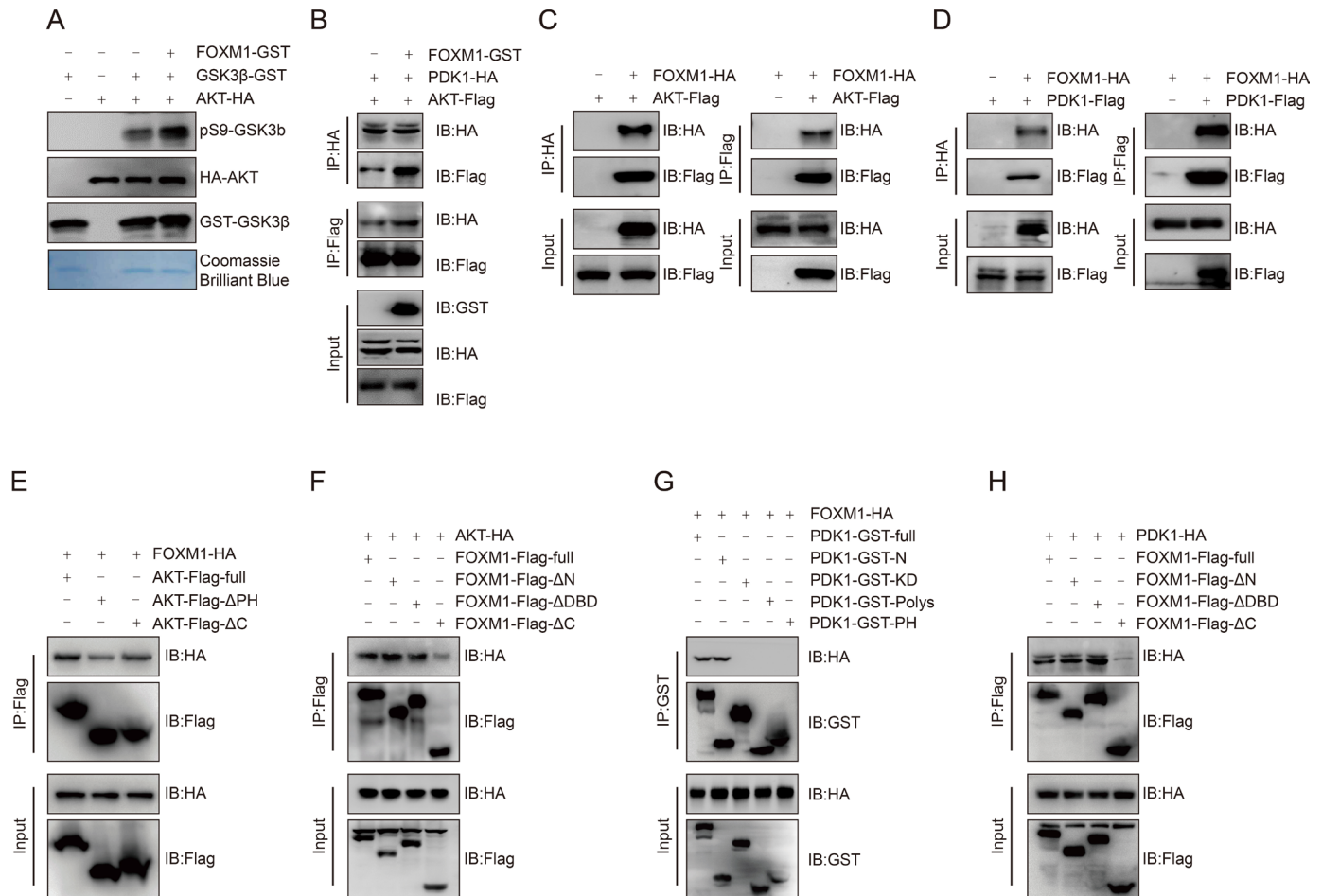


Figure 7 FOXM1 facilitates AKT activation through the enhancement of the interaction between PDK1 and AKT. (A) AKT in vitro kinase assays were performed with immuno-purified AKT kinase from HEK293T cells transfected with a control or FOXM1 overexpression plasmid, and the bacterially purified GST-GSK3 β was used as the substrate. (B) HEK293T cells were transfected with PDK1-HA and AKT-Flag with control or FOXM1-GST plasmids, then Co-IP assays were performed using HA and Flag antibodies. (C–H) HEK293T cells were transfected with various combinations of FOXM1, AKT, PDK1, and their respective mutant constructs. Co-IP assays were then conducted using the appropriate tag antibodies. Co-IP, co-immunoprecipitation.

lines (online supplemental figure S8H, I). Half-life assays showed that orlistat extended the half-life of STAT1 protein (figure 8L). To investigate the mechanism of orlistat-stabilized STAT1 protein, we performed a thermal shift assay that confirmed orlistat enhanced the thermal stability of STAT1 (figure 8M). Furthermore, the results from SPR assay validated that orlistat can bind to STAT1 with a K_D of 24.23 μ M (figure 8N,O). Taken together, we reasoned that orlistat upregulates the expression of type I IFNs and ISGs, promotes antigen-presenting gene expression by directly binding to STAT1 protein, stabilizing STAT1 protein, and activating the STAT1 signaling pathway. Thus, these results together suggest that orlistat reduces PD-L1 protein levels by blocking the AKT/FOXO3a/FOXM1 signaling pathway and promotes ISGs and MHC-I to facilitate ICB therapy (figure 8P).

PD-L1 is negatively correlated with FOXO3a expression in gastric cancer tissues

Next, we analyzed the relationship between PD-L1 and FOXO3a in clinical tissues of patients with gastric cancer.

According to immunofluorescence results, FOXO3a and CD8a were significantly less expressed in the tumor while PD-L1 was highly expressed (online supplemental figure S8A). Interestingly, online supplemental figure S8B shows a negative correlation between the expression of FOXO3a and PD-L1 proteins, indicating the possibility of a FOXO3a-PD-L1 pathway in gastric cancer tissues. The receiver operating characteristic (ROC) curves indicated that either FOXO3a or PD-L1 expression might be used to predict the prognosis of a patient (online supplemental figure S8C, D). Moreover, FOXO3a expression was strongly correlated with survival probability, but PD-L1 expression was correlated with a poorer prognosis (online supplemental figure S8E, F). The group with low FOXO3a expression but high PD-L1 expression had the shortest survival time when both of these levels were used for survival time analysis (online supplemental figure S8G). The inverse correlation between PD-L1 and FOXO3a expression was also observed in the gastric cancer cohort GSE66229 (online supplemental figure S8H).

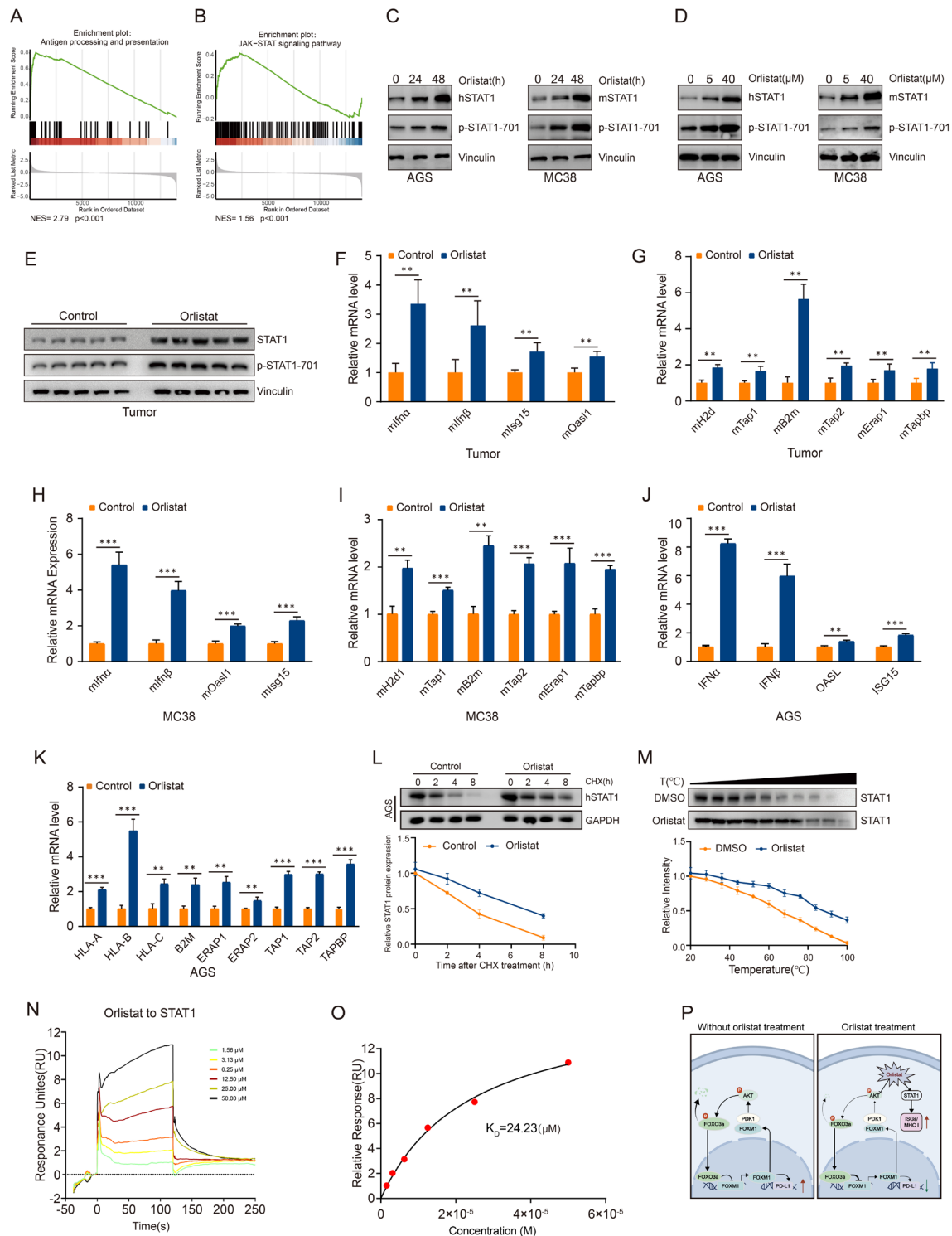


Figure 8 Orlistat upregulates ISGs and MHC-I through activating the STAT1 pathway. (A) Gene set enrichment plots of the antigen processing and presentation hallmarks. (B) Gene set enrichment plots of the JAK-STAT signaling pathway hallmarks. (C–E) WB analysis of Y701-phosphorylated STAT1 (p-STAT1-701) and total STAT1 in AGS and MC38 cells at different times (C) and concentrations (D) after orlistat administration, and tumors collected from mice-bearing subcutaneous MC38 tumors with or without orlistat treatment (E). (F–K) Quantitative PCR analysis of mRNA expression of IFN α , IFN β , and ISGs or antigen processing and presentation genes in purified MC38 syngeneic tumors cells treated with control or orlistat (F), MC38 (H, I), and AGS (J, K) cell lines. (L) IB analysis and quantitative data of STAT1 in DMSO control vs orlistat-treated cells. AGS cells were treated with cycloheximide (CHX) 100 mg/mL, and collected at the indicated times. (M) Orlistat administration (40 μ M) increased the thermal stability of STAT1 protein as determined by thermal stability shift assay (n=3). (N, O) SPR sensorgrams (N) and steady-state curves (O) for the orlistat analyte (2-fold dilutions; 50–1.56 μ M) binding to the STAT1 protein ligand. (P) Schematic diagram depicting orlistat-mediated inhibition of PD-L1 expression in gastric cancer and colon cancer cells and promoting the expression of ISGs and MHC-I **p<0.01, ***p<0.001.

PD-L1 is positively correlated with FOXM1 expression in gastric cancer tissues

In 97 gastric cancer patient tissues, we found a strong positive correlation between FOXM1 expression and PD-L1 expression (online supplemental figure S9A)(online supplemental figure S9B). Immunofluorescence staining indicated that FOXM1 and PD-L1 levels were significantly upregulated in tumor tissues and CD8a was downregulated, consistent with the results presented in (online supplemental figure S9B) online supplemental figure S8A. Furthermore, ROC analysis revealed that FOXM1 and PD-L1 were good predictive markers for survival in gastric cancer (area under the ROC curve (AUC)-FOXM1 0.8736, AUC-PD-L1 0.8517) (online supplemental figure S9C,D) (online supplemental figure C, D). Thus, FOXM1 and PD-L1 were clinically relevant in gastric cancer. Analysis of survival time showed that excessive expression of FOXM1 or PD-L1 was linked with a poor prognosis (online supplemental figure S9E, F), whereas high levels of both genes were related with the poorest prognosis (online supplemental figure S9G). Using the GSE66229 gastric cancer database, we evaluated the correlation between FOXM1 expression, PD-L1 expression, and CD8 expression. The results showed a positive correlation in mRNA expression of FOXM1 and PD-L1, as well as a negative correlation between FOXM1 and CD8 (online supplemental figure S9H, I). Collectively, these results support the view that FOXM1-mediated PD-L1 signaling plays an essential role in cancer.

DISCUSSION

Cotargeting CTLA-4 and PD-1/PD-L1 immune checkpoints is currently regarded as the most effective cancer immunotherapy, due to their distinct effects on different phases of T-cell activation.^{3 16 49} Our results indicate that orlistat can improve the efficacy of CTLA-4 antibody by downregulating PD-L1 expression on tumor cells and increasing ISGs and MHC-I expression. Specifically, orlistat administration reduces PD-L1 mRNA and protein levels via regulating AKT/FOXO3a/FOXM1 signaling, and increases ISGs and antigen presentation genes expression by directly binding to STAT1 protein to stabilize STAT1 protein and activating STAT1 pathway. Meanwhile, we also extend our understanding of the positive feedback loop of the AKT-FOXO3a-FOXM1 axis. On the one hand, FOXO3a directly interacts with FOXM1 promoter to transcriptionally regulate FOXM1, and on the other hand, FOXM1 promotes FOXO3a phosphorylation and subsequent degradation by promoting the interaction between PDK1 and AKT, leading to the activation of AKT. Collectively, orlistat combined with anti-CTLA-4 is a potential new therapeutic strategy for cancer treatment.

AKT plays a pivotal role in multiple cellular processes such as cell proliferation, survival, growth, apoptosis, and glycogen metabolism. It has been regarded as an attractive target in cancer treatment. Consistent with earlier

results that AKT activation can be affected by enhancing the PDK1-AKT interaction,^{44 50–52} our work is the first to report that FOXM1 acts a scaffold protein to promote complex formation between PDK1 and AKT. Additionally, we report a novel negative post-transcriptional regulation of FOXO3a by FOXM1 via activation of AKT signaling. Targeting dysregulated proteins in this feedback loop should offer a novel strategy for anticancer drug development.

Orlistat is a multitargeted agent for cancer therapy.⁵³ Here, we provide strong evidence that the AKT/FOXO3a/FOXM1 axis is the target of orlistat. In addition, there are reports that AKT promotes PD-L1 transcription via activation of the mTOR or NF- κ B axis,^{54 55} and additional signaling pathways also regulate PD-L1 expression such as MAPK and Notch signaling.^{56–58} Inhibition of the MAPK prevented both EGF-induced and IFN- γ -induced PD-L1 mRNA and protein upregulation in lung adenocarcinoma cells.⁵⁶ PD-L1 overexpression on breast CSCs is partly mediated by the Notch3/mTOR axis. In our research, orlistat can directly bind to STAT1, stabilize STAT1 protein, and activate the IFN-STAT1 signaling, which promotes the T cell infiltration to kill tumor cells. Previous reports have shown that the interferon signaling pathway promotes the expression of PD-L1.⁵⁹ However, orlistat downregulates PD-L1 while promoting the IFN-STAT1 signaling pathway, likely because orlistat's effects on the AKT/FOXO3a/FOXM1 axis are more pronounced, leading to an overall downregulation of PD-L1.

Nevertheless, we found that the orlistat-induced decrease in PD-L1 expression was almost abolished with either knockdown of FOXO3a or knockout of FOXM1, respectively. It is also worth mentioning that thoughtful dose and schedule regimens may have to be considered as AKT is involved in T cell activation.⁶⁰

Our experiments demonstrate that orlistat downregulates PD-L1 and activates IFN-STAT1 signaling to enhance the antitumor effect of CTLA-4 antibody. However, our study still has some limitations. First, there is a lack of clinical data on the use of orlistat in patients with cancer receiving CTLA-4 antibody. Further research and validation are needed to determine its clinical application prospects. Second, thermal shift assays provided preliminary evidence for the binding between orlistat and AKT protein; more molecular biological assays are still needed for further illustration. Third, we found orlistat activates IFN-STAT1 signaling, but without further analysis of the specific domain, as well as the potential crosstalk between AKT-FOXO3a-FOXM1 and IFN-STAT1 pathways.

Overall, our studies revealed that orlistat, an FDA-approved agent used for the treatment of obesity, is functionally associated with the reduced expression of PD-L1 and increased expression of antigen processing and presentation genes in gastric and colon cancer to sensitize tumors to ICB therapies. Our results may yield insights into the anticancer effects of orlistat and benefit the development of cancer immunotherapies.

Acknowledgements We thank Dr Jianping Guo and Dr Haixia Long for their helpful suggestions.

Contributors CH, SY and XZ devised, coordinated, and supervised the project. QT, JL, LZ and SZ performed all the experiments with the help from WH, LH, GH, and LW. QT, JL, SY, and CH analyzed the data, wrote and revised the manuscript. SZ, SY and CH provided the funding. All authors read and approved the manuscript. CH is the guarantor of the study.

Funding National Natural Science Foundation of China (81972304)

Competing interests No, there are no competing interests.

Patient consent for publication Not applicable.

Ethics approval This study involves human participants and was approved by Shanghai Outdo Biotech Company (SHYJS-CP-1710001). Participants gave informed consent to participate in the study before taking part.

Provenance and peer review Not commissioned; externally peer reviewed.

Data availability statement Data are available in a public, open access repository. Data are available on reasonable request. Not applicable.

Supplemental material This content has been supplied by the author(s). It has not been vetted by BMJ Publishing Group Limited (BMJ) and may not have been peer-reviewed. Any opinions or recommendations discussed are solely those of the author(s) and are not endorsed by BMJ. BMJ disclaims all liability and responsibility arising from any reliance placed on the content. Where the content includes any translated material, BMJ does not warrant the accuracy and reliability of the translations (including but not limited to local regulations, clinical guidelines, terminology, drug names and drug dosages), and is not responsible for any error and/or omissions arising from translation and adaptation or otherwise.

Open access This is an open access article distributed in accordance with the Creative Commons Attribution Non Commercial (CC BY-NC 4.0) license, which permits others to distribute, remix, adapt, build upon this work non-commercially, and license their derivative works on different terms, provided the original work is properly cited, appropriate credit is given, any changes made indicated, and the use is non-commercial. See <http://creativecommons.org/licenses/by-nc/4.0/>.

ORCID iD

Changjiang Hu <http://orcid.org/0000-0002-9883-9239>

REFERENCES

- Chowell D, Yoo S-K, Valero C, *et al.* Improved prediction of immune checkpoint blockade efficacy across multiple cancer types. *Nat Biotechnol* 2022;40:499–506.
- He X, Xu C. Immune checkpoint signaling and cancer immunotherapy. *Cell Res* 2020;30:660–9.
- Sharma P, Allison JP. The future of immune checkpoint therapy. *Science* 2015;348:56–61.
- Morad G, Helmink BA, Sharma P, *et al.* Hallmarks of response, resistance, and toxicity to immune checkpoint blockade. *Cell* 2021;184:5309–37.
- Zhou CB, Zhou YL, Fang JY. Gut Microbiota in Cancer Immune Response and Immunotherapy. *Trends Cancer* 2021;7:647–60.
- Ugai T, Zhao M, Shimizu T, *et al.* Association of *PIK3CA* mutation and PTEN loss with expression of CD274 (PD-L1) in colorectal carcinoma. *Oncoimmunology* 2021;10:1956173.
- Bockmayr M, Mohme M, Klauschen F, *et al.* Subgroup-specific immune and stromal microenvironment in medulloblastoma. *Oncoimmunology* 2018;7:e1462430.
- Castagnoli L, Cancila V, Cordoba-Romero SL, *et al.* WNT signaling modulates PD-L1 expression in the stem cell compartment of triple-negative breast cancer. *Oncogene* 2019;38:4047–60.
- Topper MJ, Vaz M, Chiappinelli KB, *et al.* Epigenetic Therapy Ties MYC Depletion to Reversing Immune Evasion and Treating Lung Cancer. *Cell* 2017;171:1284–300.
- Gutzmer R, Stroyakovskiy D, Gogas H, *et al.* Atezolizumab, vemurafenib, and cobimetinib as first-line treatment for unresectable advanced BRAF^{V600} mutation-positive melanoma (IMspire150): primary analysis of the randomised, double-blind, placebo-controlled, phase 3 trial. *Lancet* 2020;395:1835–44.
- Seguin F, Carvalho MA, Bastos DC, *et al.* The fatty acid synthase inhibitor orlistat reduces experimental metastases and angiogenesis in B16-F10 melanomas. *Br J Cancer* 2012;107:977–87.
- Ghoneum A, Abdulfattah AY, Warren BO, *et al.* Redox Homeostasis and Metabolism in Cancer: A Complex Mechanism and Potential Targeted Therapeutics. *Int J Mol Sci* 2020;21:3100.
- Kridel SJ, Axelrod F, Rozenkrantz N, *et al.* Orlistat is a novel inhibitor of fatty acid synthase with antitumor activity. *Cancer Res* 2004;64:2070–5.
- de Almeida LY, Mariano FS, Bastos DC, *et al.* The antimetastatic activity of orlistat is accompanied by an antitumoral immune response in mouse melanoma. *Cancer Chemother Pharmacol* 2020;85:321–30.
- Jie M, Wu Y, Gao M, *et al.* CircMRPS35 suppresses gastric cancer progression via recruiting KAT7 to govern histone modification. *Mol Cancer* 2020;19:56.
- Rotte A. Combination of CTLA-4 and PD-1 blockers for treatment of cancer. *J Exp Clin Cancer Res* 2019;38:255.
- Ceeraz S, Nowak EC, Noelle RJ. B7 family checkpoint regulators in immune regulation and disease. *Trends Immunol* 2013;34:556–63.
- Bolandi N, Derakhshani A, Hemmat N, *et al.* The Positive and Negative Immunoregulatory Role of B7 Family: Promising Novel Targets in Gastric Cancer Treatment. *Int J Mol Sci* 2021;22:10719.
- Shahid M, Kim M, Jin P, *et al.* S-Palmitoylation as a Functional Regulator of Proteins Associated with Cisplatin Resistance in Bladder Cancer. *Int J Biol Sci* 2020;16:2490–505.
- Ciocoloni G, Aquino A, Notarnicola M, *et al.* Fatty acid synthase inhibitor orlistat impairs cell growth and down-regulates PD-L1 expression of a human T-cell leukemia line. *J Chemother* 2020;32:30–40.
- Fan Z, Wu C, Chen M, *et al.* The generation of PD-L1 and PD-L2 in cancer cells: From nuclear chromatin reorganization to extracellular presentation. *Acta Pharm Sin B* 2022;12:1041–53.
- Sun C, Mezzadra R, Schumacher TN. Regulation and Function of the PD-L1 Checkpoint. *Immunity* 2018;48:434–52.
- Yi M, Niu M, Xu L, *et al.* Regulation of PD-L1 expression in the tumor microenvironment. *J Hematol Oncol* 2021;14:10.
- Madhi H, Lee J-S, Choi YE, *et al.* FOXM1 Inhibition Enhances the Therapeutic Outcome of Lung Cancer Immunotherapy by Modulating PD-L1 Expression and Cell Proliferation. *Adv Sci (Weinh)* 2022;9:e2202702.
- Wu A, Wu Q, Deng Y, *et al.* Loss of VGLL4 suppresses tumor PD-L1 expression and immune evasion. *EMBO J* 2019;38:e99506.
- Lam EW-F, Brosens JJ, Gomes AR, *et al.* Forkhead box proteins: tuning forks for transcriptional harmony. *Nat Rev Cancer* 2013;13:482–95.
- Yao S, Fan L-N, Lam E-F. The FOXO3-FOXM1 axis: A key cancer drug target and a modulator of cancer drug resistance. *Semin Cancer Biol* 2018;50:77–89.
- Pham TH, Page YL, Percevault F, *et al.* Apigenin, a Partial Antagonist of the Estrogen Receptor (ER), Inhibits ER-Positive Breast Cancer Cell Proliferation through Akt/FOXM1 Signaling. *Int J Mol Sci* 2021;22:470.
- Yung MMH, Chan DW, Liu VWS, *et al.* Activation of AMPK inhibits cervical cancer cell growth through AKT/FOXO3a/FOXM1 signaling cascade. *BMC Cancer* 2013;13:327.
- Karadedou CT, Gomes AR, Chen J, *et al.* FOXO3a represses VEGF expression through FOXM1-dependent and -independent mechanisms in breast cancer. *Oncogene* 2012;31:1845–58.
- McGovern UB, Francis RE, Peck B, *et al.* 2009 Gefitinib (Iressa) represses foxm1 expression via foxo3a in breast cancer. *Mol Cancer Ther*.
- Liu Y, Ao X, Ding W, *et al.* Critical role of FOXO3a in carcinogenesis. *Mol Cancer* 2018;17:104.
- Brunet A, Bonni A, Zigmund MJ, *et al.* Akt promotes cell survival by phosphorylating and inhibiting a Forkhead transcription factor. *Cell* 1999;96:857–68.
- Yang J-Y, Zong CS, Xia W, *et al.* ERK promotes tumorigenesis by inhibiting FOXO3a via MDM2-mediated degradation. *Nat Cell Biol* 2008;10:138–48.
- Greer EL, Oskoui PR, Banko MR, *et al.* The energy sensor AMP-activated protein kinase directly regulates the mammalian FOXO3 transcription factor. *J Biol Chem* 2007;282:30107–19.
- Song M, Bode AM, Dong Z, *et al.* AKT as a Therapeutic Target for Cancer. *Cancer Res* 2019;79:1019–31.
- Hoxhaj G, Manning BD. The PI3K-AKT network at the interface of oncogenic signalling and cancer metabolism. *Nat Rev Cancer* 2020;20:74–88.
- Liu R, Chen Y, Liu G, *et al.* PI3K/AKT pathway as a key link modulates the multidrug resistance of cancers. *Cell Death Dis* 2020;11.
- Dunn GP, Koebel CM, Schreiber RD. Interferons, immunity and cancer immunoeediting. *Nat Rev Immunol* 2006;6:836–48.
- Parker BS, Rautela J, Hertzog PJ. Antitumour actions of interferons: implications for cancer therapy. *Nat Rev Cancer* 2016;16:131–44.

- 41 Jhunjhunwala S, Hammer C, Delamarre L. Antigen presentation in cancer: insights into tumour immunogenicity and immune evasion. *Nat Rev Cancer* 2021;21:298–312.
- 42 Leibowitz MS, Srivastava RM, Andrade Filho PA, et al. SHP2 is overexpressed and inhibits pSTAT1-mediated APM component expression, T-cell attracting chemokine secretion, and CTL recognition in head and neck cancer cells. *Clin Cancer Res* 2013;19:798–808.
- 43 Jiang H, Li Y, Shen M, et al. Interferon- α promotes MHC I antigen presentation of islet β cells through STAT1-IRF7 pathway in type 1 diabetes. *Immunology* 2022;166:210–21.
- 44 Guo X, Ma P, Li Y, et al. RNF220 mediates K63-linked polyubiquitination of STAT1 and promotes host defense. *Cell Death Differ* 2021;28:640–56.
- 45 Darnell JE, JrIM, Stark GR. Jak-STAT pathways and transcriptional activation in response to IFNs and other extracellular signaling proteins. *Science* 1994;264:1415–21.
- 46 Jiao Z, Li W, Xiang C, et al. IRF11 synergizes with STAT1 and STAT2 to promote type I IFN production. *Fish Shellfish Immunol* 2024;150:109656.
- 47 Stark GR, Darnell JE Jr. The JAK-STAT pathway at twenty. *Immunity* 2012;36:503–14.
- 48 Tani T, Mathsyaraja H, Campisi M, et al. TREX1 Inactivation Unleashes Cancer Cell STING-Interferon Signaling and Promotes Antitumor Immunity. *Cancer Discov* 2024;14:752–65.
- 49 Zhang J, Zhang G, Zhang W, et al. Loss of RBMS1 promotes anti-tumor immunity through enabling PD-L1 checkpoint blockade in triple-negative breast cancer. *Cell Death Differ* 2022;29:2247–61.
- 50 Higuchi M, Onishi K, Kikuchi C, et al. Scaffolding function of PAK in the PDK1-Akt pathway. *Nat Cell Biol* 2008;10:1356–64.
- 51 Huang L, Zhang X-O, Rozen EJ, et al. PRMT5 activates AKT via methylation to promote tumor metastasis. *Nat Commun* 2022;13.
- 52 Jiang Q, Zhang X, Dai X, et al. S6K1-mediated phosphorylation of PDK1 impairs AKT kinase activity and oncogenic functions. *Nat Commun* 2022;13:1548.
- 53 Schcolnik-Cabrera A, Chávez-Blanco A, Domínguez-Gómez G, et al. Orlistat as a FASN inhibitor and multitargeted agent for cancer therapy. *Expert Opin Investig Drugs* 2018;27:475–89.
- 54 Lastwika KJ, Wilson W III, Li QK, et al. Control of PD-L1 Expression by Oncogenic Activation of the AKT–mTOR Pathway in Non–Small Cell Lung Cancer. *Cancer Res* 2016;76:227–38.
- 55 Chen J, Jiang CC, Jin L, et al. Regulation of PD-L1: a novel role of pro-survival signalling in cancer. *Ann Oncol* 2016;27:409–16.
- 56 Stutvoet TS, Kol A, de Vries EG, et al. MAPK pathway activity plays a key role in PD-L1 expression of lung adenocarcinoma cells. *J Pathol* 2019;249:52–64.
- 57 Mansour FA, Al-Mazrou A, Al-Mohanna F, et al. PD-L1 is overexpressed on breast cancer stem cells through notch3/mTOR axis. *Oncimmunology* 2020;9:1729299.
- 58 Böttcher M, Bruns H, Völkl S, et al. Control of PD-L1 expression in CLL-cells by stromal triggering of the Notch-c-Myc-EZH2 oncogenic signaling axis. *J Immunother Cancer* 2021;9:e001889.
- 59 Garcia-Diaz A, Shin DS, Moreno BH, et al. Interferon Receptor Signaling Pathways Regulating PD-L1 and PD-L2 Expression. *Cell Rep* 2017;19:1189–201.
- 60 Herrero-Sánchez MC, Rodríguez-Serrano C, Almeida J, et al. Targeting of PI3K/AKT/mTOR pathway to inhibit T cell activation and prevent graft-versus-host disease development. *J Hematol Oncol* 2016;9:113.